Arginine Methyltransferase PRMT5 Methylates and Destabilizes Mxi1 to Confer Radioresistance in Lung Cancer

Xijie Yang
Wuhan Union Hospital
Zhen Zeng
Wuhan Union Hospital
Xiaohua Jie
Wuhan Union Hospital
Ye Wang
Wuhan Union Hospital
Jun Han
Wuhan Union Hospital
Zhikun Zheng
Wuhan Union Hospital
Jinsong Li
Wuhan Union Hospital
Hongli Liu
Wuhan Union Hospital
Xiaorong Dong
Wuhan Union Hospital
Gang Wu
Wuhan Union Hospital
Shuangbing Xu (xsb723@hust.edu.cn)
Wuhan Union hospital

Research

Keywords: PRMT5, Mxi1, Methylation, Radioresistance, Lung cancer

Posted Date: November 15th, 2021

DOI: https://doi.org/10.21203/rs.3.rs-1061482/v1

Abstract

Background

Radioresistance is regarded as the main cause of local recurrence and distant metastasis in lung cancer. However, the underlying mechanisms of radioresistance remain incompletely understood. This study investigates the roles and regulatory mechanisms of arginine methyltransferase PRMT5 in lung cancer radioresistance.

Methods

Immunoprecipitation assay and GST pulldown were used to detect the protein-protein interaction. The methylation of Mxi1 was determined by *in vivo* and *in vitro* arginine methylation assays. *In vivo* ubiquitination and CHX chase assays were performed to examine the stability of Mxi1. The biological effects of PRMT5 and its specific inhibitor EPZ015666 in lung cancer were evaluated both *in vitro* and *in vivo*.

Results

We show that the arginine methyltransferase PRMT5 interacts with and methylates Mxi1, which promotes the binding of the β-Trcp ligase to Mxi1, facilitating the ubiquitination and degradation of Mxi1 in lung cancer. Furthermore, genetic blockade of PRMT5 impairs DNA damage repair and enhances lung cancer radiosensitivity *in vitro* and *in vivo*, and these phenotypes are partially reversed by Mxi1 silencing. More importantly, pharmacological inhibition of PRMT5 with the specific inhibitor EPZ015666 leads to extraordinary radiosensitization *in vitro* and *in vivo* in lung cancer.

Conclusions

Our data indicate that PRMT5 methylates and destabilizes Mxi1 to confer radioresistance, suggesting that PRMT5 may be a promising radiosensitization target in lung cancer.

Background

Protein arginine methylation is increasingly considered to be a pivotal posttranslational modification that is carried out by protein arginine methyltransferases (PRMTs) that catalyze the monomethylation and dimethylation of the guanidium group of arginine residues, with S-adenosyl methionine (SAM) serving as a methyl group donor [1-3]. PRMT5, a type II arginine methyltransferase, catalyzes the symmetrical dimethylation of arginine residues within target proteins orchestrating a variety of cellular processes, including cell growth and proliferation, mRNA splicing, DNA damage repair, T cell development and immunity, cellular metabolism and inflammation [4-8]. Human PRMT5 is commonly activated and overexpressed in several types of cancer, including leukemia, lymphoma and solid tumors [9, 10], suggesting that PRMT5 may be an attractive target for anticancer therapy. In addition, PRMT5 has been

reported to directly control the arginine methylation of histone and nonhistone proteins, including p53, KLF4, TDP1 and KLF5 [11-14], thereby influencing protein stability and function.

On the basis of the PRMT5 molecular structure, a variety of PRMT5 inhibitors have been developed, among which EPZ015666 (GSK3235025) is an efficient and specific commercial inhibitor that has been used in preclinical research on hematological tumors and solid tumors [15, 16]. For example, in a mantle cell lymphoma transplantation tumor model, EPZ015666 can inhibit tumor formation in a dose-dependent manner [17]. Moreover, EPZ015666 inhibits the tumorigenesis of multiple myeloma and acute myeloid leukemia *in vivo* and *in vitro* [18, 19]. In addition, in the context of malignant gliomas, EPZ015666 regulates cell senescence and cell cycle arrest to suppress the formation of glioblastoma [20]. Recent evidence has shown that EPZ015666 can reduce the proliferation of triple-negative breast cancer cells and significantly delay tumor progression [21]. These findings indicate that the PRMT5-specific inhibitor EPZ015666 has a potential antitumor effect. However, no reports have indicated whether EPZ015666 has a radiosensitizing effect on human cancers.

Mxi1 acts as an antagonist of Myc by combining with MAX to form a heterodimer that binds to the E-box site of a downstream target gene of Myc [22]. Therefore, Mxi1 is thought to negatively regulate the transcriptional activity of Myc. Accumulating evidence has shown that Mxi1 plays crucial roles in orchestrating a series of biological functions, including cell growth and apoptosis, the cell cycle, production of reactive oxygen species and radiosensitivity [23, 24]. Mxi1 is also involved in tumorigenesis in prostate cancer and acute myeloid leukemia [25, 26]. Our previous study demonstrated that phosphorylation of Mxi1 by the S6K1 kinase promotes its recognition and degradation by β-Trcp ligase [27]. In addition, we discovered that the E2/E3 ubiquitin ligase UBE2O destabilizes Mxi1 to confer radioresistance in lung cancer [28]. Additional mechanisms that may regulate Mxi1 stability remain to be revealed.

In this study, we identify the arginine methyltransferase PRMT5 as a novel binding partner of Mxi1. PRMT5 contributes to the ubiquitination and degradation of Mxi1 by engaging in the posttranslational arginine methylation of Mxi1. We demonstrate that inhibition of PRMT5 suppresses DNA damage repair and results in radiosensitization in lung cancer.

Materials And Methods

Cell culture and plasmids

H1299, A549, H1975, HCC827, H292 and HEK293T cell lines were purchased from ATCC and cultured in Gibco RPMI-1640 or DMEM with 10% FBS and 100 μg/mL streptomycin and penicillin in 5% CO2 at 37 °C. PRMT5 and Mxi1 plasmids were generated by subcloning constructs into a pDNOR201 entry vector that were then transferred to a destination vector with SFB, HA, Myc, or GST tags by Gateway Technology (Invitrogen).

Antibodies and reagents

Anti-PRMT5 antibody (ab109451) and anti-Rad51 antibody (ab133534) were purchased from Abcam. Anti-Mxi1 antibody (HPA035319), anti-histone H2A antibody (ABE327), anti-Flag antibody (F1804), EPZ015666 (SML1421) and cycloheximide (CHX, 01810) were purchased from Sigma-Aldrich. Anti-GAPDH (A19056) antibody was obtained from ABclonal. Anti-Myc (sc-40) antibody was purchased from Santa Cruz Biotechnology. Anti-GST (#2624) and anti-HA (#3724) antibodies were purchased from Cell Signaling Technology. Recombinant SAM (B9003S) and human histone H2A (M2502S) were obtained from New England Biolabs. Recombinant His-Mxi1 protein was obtained from Abnova. The proteasome inhibitor MG132 (#474790) and rabbit polyclonal anti-symmetric dimethyl arginine (SDMA, 07-413) antibody were purchased from Millipore.

SiRNAs transfection

SiRNAs (short interfering RNAs) transfection was conducted as described previously [27, 28]. Briefly, cells were transfected with the indicated siRNAs with Lipofectamine RNAiMAX (Invitrogen) for 48 h. Then, cells were collected and analyzed by immunoblotting. The following siRNA sequences targeted PRMT5 were used:

si-PRMT5#1: 5-GGACCTGAGAGATGATATA-3 [29] and

si-PRMT5#2: 5-GAGGATTGCAGTGGCTCTT-3 [29].

Establishing stable PRMT5-knockout (KO) cell lines

Stable KO PRMT5 cell lines were established by transfecting HEK293T cells with pSPAX2 and pMD2G packaging plasmids and a short hairpin RNA (shRNA). Forty-eight hours after transfection, the lentiviral supernatants were collected and filtered through a 0.45 μm filter. Lung cancer cells were infected with these lentiviral supernatants for 48 h with polybrene (10 μg/mL). Stable cells were screened with 2 μg/ml puromycin, and verified by Western blotting. The following shRNAs against PRMT5 were used:

sh-PRMT5 #1: 5-AGGGACTGGAATACGCTAATT-3 [30] and

sh-PRMT5 #2: 5-GCGGATAAAGCTGTATGCTGT-3 [30].

Western blotting and co-immunoprecipitation (co-IP)

Cell lysates were prepared with NETN buffer (150 mM NaCl, 0.5 mM EDTA, 20 mM Tris–HCl at pH 8.0, and 0.5% NP-40), seperated by SDS-PAGE according to the manufacturer's procedure (Bio-Rad). The membranes were incubated overnight at 4 °C with appropriate primary antibodies. After washing 3 times, the membranes were incubated with the corresponding secondary antibodies for 1 h and visualized by the ECL system (Bio-Rad). For exogenous co-immunoprecipitation, cell lysates were incubated overnight with S-protein agarose (Novagen) at 4 °C. For endogenous binding, cell supernatants were incubated with anti-PRMT5 antibody and protein A/G agarose (Santa Cruz Biotechnology).

GST pull-down assay

Purified GST-only or GST-PRMT5 proteins were immobilized on Glutathione-Sepharose 4B beads (GE Healthcare) and mixed with the lysates of HEK293T cells that had been transfected with the SFB-Mxi1 plasmid; the mixture was incubated for 2 h at 4 °C. The samples were then analyzed by immunoblotting.

In vitro arginine methylation assay

Recombinant GST-PRMT5 and His-Mxi1 or Histone H2A proteins were mixed with SAM and incubated in 1× PBS buffer at 37 °C for 2 h. The reaction was stopped by adding SDS protein sample loading buffer and heating at 95 °C for 10 min. The samples were then analyzed by Western blotting.

In vivo ubiquitination and CHX chase assays

Cells transfected with the indicated plasmids and siRNAs were pretreated with MG132 (10 μm for 4h) before collection. Cell supernatants were incubated with S beads overnight. Ubiquitinated Mxi1 was determined by Western blotting. For the CHX chase assay, cells were cultured in a 6-well plate prior to the addition of CHX (20 μg/ml). After treatment at the indicated time points, cells were collected and subjected to immunoblotting to measure the protein levels.

Neutral comet assay

Cells were collected 4 h after irradiation (6 Gy), mixed with comet low melting agarose (LMA) at the proper proportion and spread evenly on comet slide sample wells. After maintenance at 4 °C for 15 min, the slides were immersed in a lysis solution containing lysates and incubated for 2 h, placed in precooled neutral electrophoresis buffer and electrophoresed for 1 h at a constant voltage of 21 V and 4 °C. The slides were soaked and then stained with SYBR Gold (Invitrogen) for 8 min. The olive tail moments were analyzed by CometScore 2.0 and GraphPad Prism software.

Clonogenic cell survival assay

A clonogenic cell survival assay was performed to detect the sensitivity of tumor cells to radiation. Cells of each group were plated in triplicate in a 6-well plate and then irradiated with different X-ray doses. After radiation exposure, the cells were cultured for 10-14 days. When clones were formed (a clone of ≥ 50 cells was considered a positive clone), the cells were fixed with 4% formaldehyde and treated with crystal violet solution for 30 min. The clones were counted, and a clone formation curve was drawn as described previously [31].

Immunofluorescence staining

Cells were treated, irradiated with 6 Gy, fixed with 4% paraformaldehyde, and then permeated with 0.2% Triton X-100. These cells were then blocked with 5% bovine serum albumin (BSA) and incubated with anti-Rad51 antibody overnight and secondary antibody for 1 h. Rad51 foci were visualized by a confocal microscope.

Mouse xenograft tumor model

All animal experiments were approved by The Medical Ethics Committee of Tongji Medical College, Huazhong University of Science and Technology. Four- to six-week-old BALB/c nude mice were allocated randomly into different groups and injected subcutaneously with 5×10^6 A549 cells. When the tumor volume reached approximately 130 mm^3, 10 Gy local IR or drug treatment was administered as described previously [28, 31]. EPZ015666 was administered to nude mice every two days by oral gavage. The size and weight of the tumors were monitored by a blinded reader every three days. The tumor volume was calculated as follows: volume = (length × $width^2$)/2.

Statistical analysis

Each experiment was independently repeated three times. All statistical power analysis for group comparisons were performed using Student's t-test (two-tailed). The experimental data are presented as the means ± SD unless stated otherwise. $P < 0.05$ was considered to be statistically significant (*$P < 0.05$, **$P < 0.01$, and ***$P < 0.001$).

Results

Mxi1 interacts with PRMT5 through the Mxi1 basic region–helix-loop-helix–leucine zipper (B-HLH-LZ) domain

Mxi1 is generally considered a tumor suppressor in human cancers. Nevertheless, the posttranslational modifications of Mxi1 are not yet been fully understood. To this end, we previously screened Mxi1-binding proteins by tandem affinity purification (TAP) and mass spectrometry analysis and found that, in addition to the known Mxi1-binding proteins SIN3A, UBE2O, Cul1 and β-Trcp2, PRMT5 was also one of the potentially binding proteins for Mxi1 [27, 28]. To confirm the Mxi1-PRMT5 interaction, we first performed a co-IP assay and found that exogenously expressed Mxi1 was associated with exogenous PRMT5 (Fig. 1A). Then, we found that endogenous PRMT5 can form a complex with exogenously transfected SFB-tagged Mxi1 and vice versa (Fig. 1B). Furthermore, the endogenous interaction between PRMT5 and Mxi1 was observed in different lung cancer cells (Fig. 1C). **Additionally, a GST pull-down assay showed that PRMT5 directly binds to Mxi1 *in vitro* (**Fig. 1D). These results confirm that PRMT5 binds to Mxi1 *in vivo* and *in vitro*. Next, to map the domain of Mxi1 that interacts with PRMT5, different SFB-tagged deletion mutants of Mxi1 were constructed (Fig. 1E). Notably, we found that when the B-HLH-LZ domain of Mxi1 was deleted, Mxi1 failed to interact with PRMT5, suggesting that the B-HLH-LZ domain is necessary for Mxi1 binding to PRMT5 (Fig. 1F). Together, these results strongly corroborate the notion that Mxi1 **directly interacts with** PRMT5 in **cells.**

PRMT5 directly methylates Mxi1 to negatively control its protein stability

Given that PRMT5 has methyltransferase activity, we speculated that Mxil might be a methylation substrate of PRMT5. To test this hypothesis, we carried out co-IP using the an anti-SDMA antibody, which recognizes symmetrically dimethylated arginine. As expected, Mxi1 dimethylation was observed in H1299

and A549 cells (Fig. 2A). Moreover, PRMT5 depletion by siRNAs or shRNAs markedly decreased symmetric arginine dimethylation of Mxi1 (Fig. 2B, C), suggesting that Mxi1 might be symmetrically dimethylated by PRMT5 in cells. EPZ015666 has been reported to specifically inhibit PRMT5 enzymatic activity. Therefore, we treated H1299 cells with 10 μM EPZ015666 for 48 h and found that EPZ015666 suppressed the total SDMA level (Fig. 2D). Consistently, the symmetrical arginine dimethylation of Mxi1was substantially reduced when H1299 and A549 cells were treated with EPZ015666 (Fig. 2E). More importantly, an *in vitro* methylation assay indicated that PRMT5 directly dimethylates the Mxi1 protein (Fig. 2F). These data indicate that PRMT5 directly binds to and methylates Mxi1 in lung cancer.

Given that Mxi1 can be degraded by the ubiquitin-proteasome system (UPS) and because PRMT5 interacts with and methylates Mxi1, we surmised that the symmetrical arginine dimethylation of Mxi1 may modulate Mxi1 degradation through ubiquitination. To test this hypothesis, we cotransfected H1299 cells with plasmids encoding Myc-tagged PRMT5 and SFB-tagged Mxi1 and performed co-IP using S beads. As expected, ectopic expression of PRMT5 promoted the binding of Mxi1 to the β-Trcp ligase (Fig. 3A). We also found that depletion of PRMT5 led to a decreased interaction between Mxi1 and β-Trcp (Fig. 3B), indicating that PRMT5 might negatively regulate Mxi1 accumulation in cells. In line with this idea, knocking down PRMT5 by siRNAs or shRNAs greatly stabilized the Mxi1 protein in different human lung cancer cells (Fig. 3C, D). Consistently, inhibition of PRMT5 with EPZ015666 resulted in Mxi1 protein abundance in a concentration- and time-dependent manner (Fig. 3E). Our data demonstrated that PRMT5 negatively regulates Mxi1 stability in lung cancer cells. In agreement with this idea, genetic or pharmacological inhibition of PRMT5 greatly decreased Mxi1 polyubiquitination *in vivo* (Fig. 3F-H). Furthermore, the half-life of endogenous Mxi1 was dramatically extended in PRMT5-deficient cells (Fig. 3I). In summary, these results indicate that PRMT5 methylates Mxi1 to facilitate Mxi1 ubiquitin-mediated degradation in lung cancer.

PRMT5 knockdown enhances lung cancer radiosensitivity *in vitro* and *in vivo*

Our previous studies have demonstrated that Mxi1 can regulate DNA damage repair and radiosensitivity in lung cancer [27, 28]. Specifically, we showed that PRMT5 methylates Mxi1 to induce its degradation; therefore, we speculated that PRMT5 might be related to the repair of IR-induced DNA damage in lung cancer. Therefore, we first performed a neutral comet assay in cells expressing two distinct PRMT5-targeting shRNAs or a control shRNA. As shown in Fig. 4A, the olive tail moment was increased in PRMT5-deficient cells. Moreover, we evaluated IR-induced Rad51 foci formation to assess DNA repair capacity and found that PRMT5 silencing reduced Rad51 recruitment to sites of DNA damage (Fig. 4B). Consistently, PRMT5-depleted H1299 and A549 cells exhibited increased sensitivity to IR (Fig. 4C). These findings indicate that loss of PRMT5 promotes DNA damage and impairs DNA repair.

To further determine the function of PRMT5 *in vivo*, we constructed an *in vivo* subcutaneous xenograft tumor model. As shown in Fig. 4D-F, PRMT5 knockdown by different shRNAs significantly reduced the growth and weight of xenograft tumors. In addition, we observed that the tumor growth and weight in the irradiated control group were profoundly lower than those in the nonirradiated control group, indicating

that the IR treatment was effective. More importantly, sh-PRMT5 groups exposed to radiation showed significantly reduced the growth and weight of xenograft tumors compared to those of the control group exposed only to radiation(Fig. 4D-F). Together, our data support that knocking down PRMT5 enhances lung cancer radiosensitivity *in vitro* and *in vivo.*

The PRMT5-specific inhibitor EPZ015666 induces an enhanced radiosensitization effect in lung cancer *in vitro* and *in vivo*

Given that PRMT5 silencing impairs radioresistance in lung cancer, we asked whether the PRMT5-specific inhibitor EPZ015666 has a similar effect. As expected, neutral comet assays showed that EPZ015666 treatment increased the comet tail moment (Fig. 5A), indicating that EPZ015666 promoted IR-induced DNA damage. Moreover, IR-induced Rad51 foci formation was significantly impaired when cells were treated with EPZ015666 (Fig. 5B). Consistently, EPZ015666 treatment sensitized cells to IR (Fig. 5C). These data suggest that the PRMT5-specific inhibitor EPZ015666 can regulate double-strand break (DSB) repair and cell survival after IR *in vitro*.

To further explore the function of the PRMT5 inhibitor EPZ015666 *in vivo*, we established a subcutaneous xenograft model and found that 100 mg/kg EPZ015666 **greatly suppressed the growth and weight of xenograft tumors, whereas** 50 mg/kg **EPZ015666** failed to have this effect (Fig. 5D-F), suggesting that EPZ015666 inhibits tumorigenesis in a concentration-dependent manner. However, 50 mg/kg EPZ015666 combined with irradiation caused a synergistic inhibitory effect on tumor growth and weight (Fig. 5G-I). In summary, these results indicate that EPZ015666 may be a promising radiosensitizer in lung cancer.

PRMT5 participates in lung cancer radioresistance in an Mxi1-dependent manner

To determine whether Mxi1 is necessary for PRMT5 to exert an effect in lung cancer, we first employed siRNAs targeting Mxi1, PRMT5 or both to knockdown target protein levels (Fig. 6A). As shown in Fig. 6B, PRMT5-deficient cells displayed an increased olive tail moment, and this phenotype was partially reversed by Mxi1 silencing. Moreover, Mxi1 knockdown partially reversed the defects in Rad51 foci formation induced by PRMT5 depletion (Fig. 6C). In addition, depletion of Mxi1 partially restored defects in PRMT5-deficient cell survival after IR (Fig. 6D). These results demonstrate that PRMT5 participates in lung cancer radioresistance by destabilizing Mxi1.

Discussion

In the current study, we provided evidence that PRMT5 interacts with and methylates Mxi1, subsequently enhancing the binding of Mxi1 to β-Trcp and thus inducing the ubiquitin-mediated degradation of Mxi1, which in turn promotes radioresistance in lung cancer. In addition, the genetic or pharmacological inhibition of PRMT5 exhibited a radiosensitization effect in lung cancer, suggesting that PRMT5 may be a novel therapeutic target for lung cancer radiotherapy.

The heterodimer formed by Mxi1 and MAX is known to bind to the E-box site of a downstream target gene of Myc, antagonizing the transcriptional activity of Myc [22]. Our previous studies have shown that Mxi1 can be phosphorylated and thus ubiquitinated and degraded by the UPS [27, 28]. However, we observed Mxi1 polyubiquitination even after the phosphorylation site was mutated, indicating that additional modifications promote Mxi1 degradation. In this study, we discovered that PRMT5 interacts with and symmetrically methylates Mxi1 in lung cancer. This interaction facilitates the binding of Mxi1 to the β-Trcp ligase, thus accelerating the degradation of Mxi1 through the UPS. These findings suggest that PRMT5 is a crucial negative modulator of Mxi1; however, the Mxi1 sites that are methylated by PRMT5 need to be further identified. Collectively, our study data not only reveal a previously unknown posttranscriptional modification of Mxi1 by PRMT5 but also establish novel crosstalk between components of protein methylation and ubiquitination that orchestrates the abundance of Mxi1 in lung cancer.

Accumulating evidence has shown that PRMT5 functions as an oncoprotein in human cancers and promotes oncogenesis [32-35]. For instance, PRMT5 interacts with EZH2 to epigenetically repress CDKN2B expression, thereby contributing to colorectal cancer progression [33]. PRMT5 is also reported to promote melanomagenesis via the SKI/SOX10 axis [32]. Additionally, the roles of PRMT5 in DNA damage repair have also been documented [36-39]. However, the functions of PRMT5 and its specific inhibitor EPZ015666 in lung cancer radioresistance remains completely unknown. In the current study, we revealed that depletion of PRMT5 enhanced the sensitivity of lung cancer cells to DNA damage, and these effects were rescued by Mxi1 silencing, indicating that Mxi1 is a key downstream effector of PRMT5 in lung cancer. Notably, PRMT5 blockade by EPZ105666 significantly increased the level of Mxi1 protein and impaired DNA damage repair in lung cancer. More importantly, the combination of low-concentration EPZ105666 and irradiation in an animal model led to an obvious synergistic effect on the growth of xenograft tumors. Our results reveal a novel role of the PRMT5-specific inhibitor EPZ105666 and provide strong preclinical evidences for the potential therapeutic application of EPZ015666 in lung cancer radiotherapy.

Conclusion

In conclusion, our study demonstrated that PRMT5 targets Mxi1 for symmetrical dimethylation, which promotes the ubiquitination and degradation of Mxi1, thus leading to lung cancer radiosensitization (Fig. 6E). These findings not only clarify the underlying mechanism by which Mxi1 is modified by PRMT5 at the posttranscriptional level but also suggest that EPZ015666 may be a potential radiosensitizer in the intervention of lung cancer.

Abbreviations

PRMT5: protein arginine methyltransferase 5; SDMA: symmetric dimethyl arginine; TAP: tandem affinity purification; DSBs: DNA double-strand breaks; UPS: ubiquitin-proteasome system; WCL: whole cell lysate; CHX: cycloheximide.

Declarations

Ethics approval and consent to participate

This study was approved by The Medical Ethics Committee of Tongji Medical College, Huazhong University of Science and Technology. Animal experiment was approved by the Animal Care and Use Committee at Tongji Medical College, Huazhong University of Science and Technology.

Consent for publication

Not applicable.

Availability of data and materials

The analyzed datasets generated during the current study are available from the corresponding author on reasonable request.

Competing interests

The authors declare that they have no competing interests.

Funding

This work was supported by the grant from the Wuhan Science and Technology Bureau (2019020701011437); the National Natural Science Foundation of China (82073351) and the Hubei Provincial Natural Science Fund for Distinguished Young Scholars (2019CFA063).

Author contributions

SX conceived and designed the study, SX and GW supervised the study, XY, ZZ and XJ performed experiments and analyzed the data, YW, JH, HL and XD provided advice and technical assistance, SX wrote the paper. All authors read and approved the final manuscript.

Acknowledgments

Not applicable.

References

1. Yang Y, Bedford MT. Protein arginine methyltransferases and cancer. Nat Rev Cancer. 2013; 13:37-50.

2. Blanc RS, Richard S. Arginine Methylation: The Coming of Age. Mol Cell. 2017;65:8-24.

3. Guccione E, Richard S. The regulation, functions and clinical relevance of arginine methylation. Nat Rev Mol Cell Biol. 2019;20:642-57.

4. Stopa N, Krebs JE, Shechter D. The PRMT5 arginine methyltransferase: many roles in development, cancer and beyond. Cell Mol Life Sci. 2015;72:2041-59.

5. Zhu F, Rui L. PRMT5 in gene regulation and hematologic malignancies. Genes Dis. 2019;6: 247-57.

6. Kim H, Kim H, Feng Y, Li Y, Tamiya H, Tocci S, et al. PRMT5 control of cGAS/STING and NLRC5 pathways defines melanoma response to antitumor immunity. Sci Transl Med. 2020;12:eaaz5683.

7. Webb LM, Sengupta S, Edell C, Piedra-Quintero ZL, Amici SA, Miranda JN, et al. Protein arginine methyltransferase 5 promotes cholesterol biosynthesis-mediated Th17 responses and autoimmunity. J Clin Invest. 2020;130:1683-98.

8. Jia Z, Yue F, Chen X, Narayanan N, Qiu J, Syed SA, et al. Protein Arginine Methyltransferase PRMT5 Regulates Fatty Acid Metabolism and Lipid Droplet Biogenesis in White Adipose Tissues. Adv Sci. 2020;7:2002602.

9. Xiao W, Chen X, Liu L, Shu Y, Zhang M, Zhong Y. Role of protein arginine methyltransferase 5 in human cancers. Biomed Pharmacother. 2019;114:108790.

10. Sengupta S, Kennemer A, Patrick K, Tsichlis P, Guerau-de-Arellano M. Protein Arginine Methyltransferase 5 in T Lymphocyte Biology. Trends Immunol. 2020;41:918-31.

11. Jansson M, Durant ST, Cho EC, Sheahan S, Edelmann M, Kessler B, et al. Arginine methylation regulates the p53 response. Nat Cell Biol. 2008;10:1431-9.

12. Hu D, Gur M, Zhou Z, Gamper A, Hung MC, Fujita N, et al. Interplay between arginine methylation and ubiquitylation regulates KLF4-mediated genome stability and carcinogenesis. Nat Commun. 2015;6:8419.

13. Rehman I, Basu SM, Das SK, Bhattacharjee S, Ghosh A, Pommier Y, et al. PRMT5-mediated arginine methylation of TDP1 for the repair of topoisomerase I covalent complexes. Nucleic Acids Res. 2018;46:5601-17.

14. Wang X, Qiu T, Wu Y, Yang C, Li Y, Du G, et al. Arginine methyltransferase PRMT5 methylates and stabilizes KLF5 via decreasing its phosphorylation and ubiquitination to promote basal-like breast cancer. Cell Death Differ. 2021;28:2931-45.

15. Wang Y, Hu W, Yuan Y. Protein Arginine Methyltransferase 5 (PRMT5) as an Anticancer Target and Its Inhibitor Discovery. J Med Chem. 2018; 61:9429-41.

16. Lin H, Wang M, Zhang YW, Tong S, Leal RA, Shetty R, et al. Discovery of Potent and Selective Covalent Protein Arginine Methyltransferase 5 (PRMT5) Inhibitors. ACS Med Chem Lett. 2019;10:1033-8.

17. Chan-Penebre E, Kuplast KG, Majer CR, Boriack-Sjodin PA, Wigle TJ, Johnston LD, et al. A selective inhibitor of PRMT5 with in vivo and in vitro potency in MCL models. Nat Chem Biol. 2015;11:432-7.

18. Gullà A, Hideshima T, Bianchi G, Fulciniti M, Kemal Samur M, Qi J, et al. Protein arginine methyltransferase 5 has prognostic relevance and is a druggable target in multiple myeloma. Leukemia. 2018;32:996-1002.

19. Serio J, Ropa J, Chen W, Mysliwski M, Saha N, Chen L, et al. The PAF complex regulation of Prmt5 facilitates the progression and maintenance of MLL fusion leukemia. Oncogene. 2018;37:450-60.

20. Braun CJ, Stanciu M, Boutz PL, Patterson JC, Calligaris D, Higuchi F, et al. Coordinated Splicing of Regulatory Detained Introns within Oncogenic Transcripts Creates an Exploitable Vulnerability in Malignant Glioma. Cancer Cell. 2017;32:411-26.

21. Vinet M, Suresh S, Maire V, Monchecourt C, Némati F, Lesage L, et al. Protein arginine methyltransferase 5: A novel therapeutic target for triple-negative breast cancers. Cancer Med. 2019;8:2414-28.

22. Grandori C, Cowley SM, James LP, Eisenman RN. The Myc/Max/Mad network and the transcriptional control of cell behavior. Annu Rev Cell Dev Biol. 2000;16:653-99.

23. Rottmann S, Lüscher B. The Mad side of the Max network: antagonizing the function of Myc and more. Curr Top Microbiol Immunol. 2006;302:63-122.

24. Cascón A, Robledo M. MAX and MYC: a heritable breakup. Cancer Res. 2012;72:3119-24.

25. Long Q, Xu J, Osunkoya AO, Sannigrahi S, Johnson BA, Zhou W, et al. Global transcriptome analysis of formalin-fixed prostate cancer specimens identifies biomarkers of disease recurrence. Cancer Res. 2014;74:3228-37.

26. Weng S, Matsuura S, Mowery CT, Stoner SA, Lam K, Ran D, et al. Restoration of MYC-repressed targets mediates the negative effects of GM-CSF on RUNX1-ETO leukemogenicity. Leukemia. 2017;31:159-69.

27. Huang Y, Hu K, Zhang S, Dong X, Yin Z, Meng R, et al. S6K1 phosphorylation-dependent degradation of Mxi1 by β-Trcp ubiquitin ligase promotes Myc activation and radioresistance in lung cancer. Theranostics. 2018;8:1286-300.

28. Huang Y, Yang X, Lu Y, Zhao Y, Meng R, Zhang S, *et al.* UBE2O targets Mxi1 for ubiquitination and degradation to promote lung cancer progression and radioresistance. Cell Death Differ. 2021;28:671-84.

29. Zhang W, Chen J, Wu M, Zhang X, Zhang M, Yue L, et al. PRMT5 restricts hepatitis B virus replication through epigenetic repression of covalently closed circular DNA transcription and interference with pregenomic RNA encapsidation. Hepatology. 2017;66:398-415.

30. Mavrakis KJ, McDonald ER 3rd, Schlabach MR, Billy E, Hoffman GR, deWeck A, et al. Disordered methionine metabolism in MTAP/CDKN2A-deleted cancers leads to dependence on PRMT5. Science. 2016;351:1208-13.

31. Jie X, Fong WP, Zhou R, Zhao Y, Zhao Y, Meng R, et al. USP9X-mediated KDM4C deubiquitination promotes lung cancer radioresistance by epigenetically inducing TGF-β2 transcription. Cell Death Differ. 2021;28:2095-111.

32. Tamiya H, Kim H, Klymenko O, Kim H, Feng Y, Zhang T, et al. SHARPIN-mediated regulation of protein arginine methyltransferase 5 controls melanoma growth. J Clin Invest. 2018;128:517-30.

33. Yang L, Ma DW, Cao YP, Li DZ, Zhou X, Feng JF, et al. PRMT5 functionally associates with EZH2 to promote colorectal cancer progression through epigenetically repressing CDKN2B expression. Theranostics. 2021;11:3742-59.

34. Luo Y, Gao Y, Liu W, Yang Y, Jiang J, Wang Y, et al. Myelocytomatosis-Protein Arginine N-Methyltransferase 5 Axis Defines the Tumorigenesis and Immune Response in Hepatocellular Carcinoma. Hepatology. 2021;74:1932-51.

35. Cai C, Gu S, Yu Y, Zhu Y, Zhang H, Yuan B, et al. PRMT5 Enables Robust STAT3 Activation via Arginine Symmetric Dimethylation of SMAD7. Adv Sci. 2021;8:2003047.

36. Hamard PJ, Santiago GE, Liu F, Karl DL, Martinez C, Man N, et al. PRMT5 Regulates DNA Repair by Controlling the Alternative Splicing of Histone-Modifying Enzymes. Cell Rep. 2018;24:2643-57.

37. Owens JL, Beketova E, Liu S, Tinsley SL, Asberry AM, Deng X, et al. PRMT5 Cooperates with pICln to Function as a Master Epigenetic Activator of DNA Double-Strand Break Repair Genes. iScience. 2020;23:100750.

38. Wei X, Yang J, Adair SJ, Ozturk H, Kuscu C, Lee KY, et al. Targeted CRISPR screening identifies PRMT5 as synthetic lethality combinatorial target with gemcitabine in pancreatic cancer cells. Proc Natl Acad Sci U S A. 2020;117:28068-79.

39. Pastore F, Bhagwat N, Pastore A, Radzisheuskaya A, Karzai A, Krishnan A, et al. PRMT5 Inhibition Modulates E2F1 Methylation and Gene-Regulatory Networks Leading to Therapeutic Efficacy in JAK2(V617F)-Mutant MPN. Cancer Discov. 2020;10:1742-57.

Figures

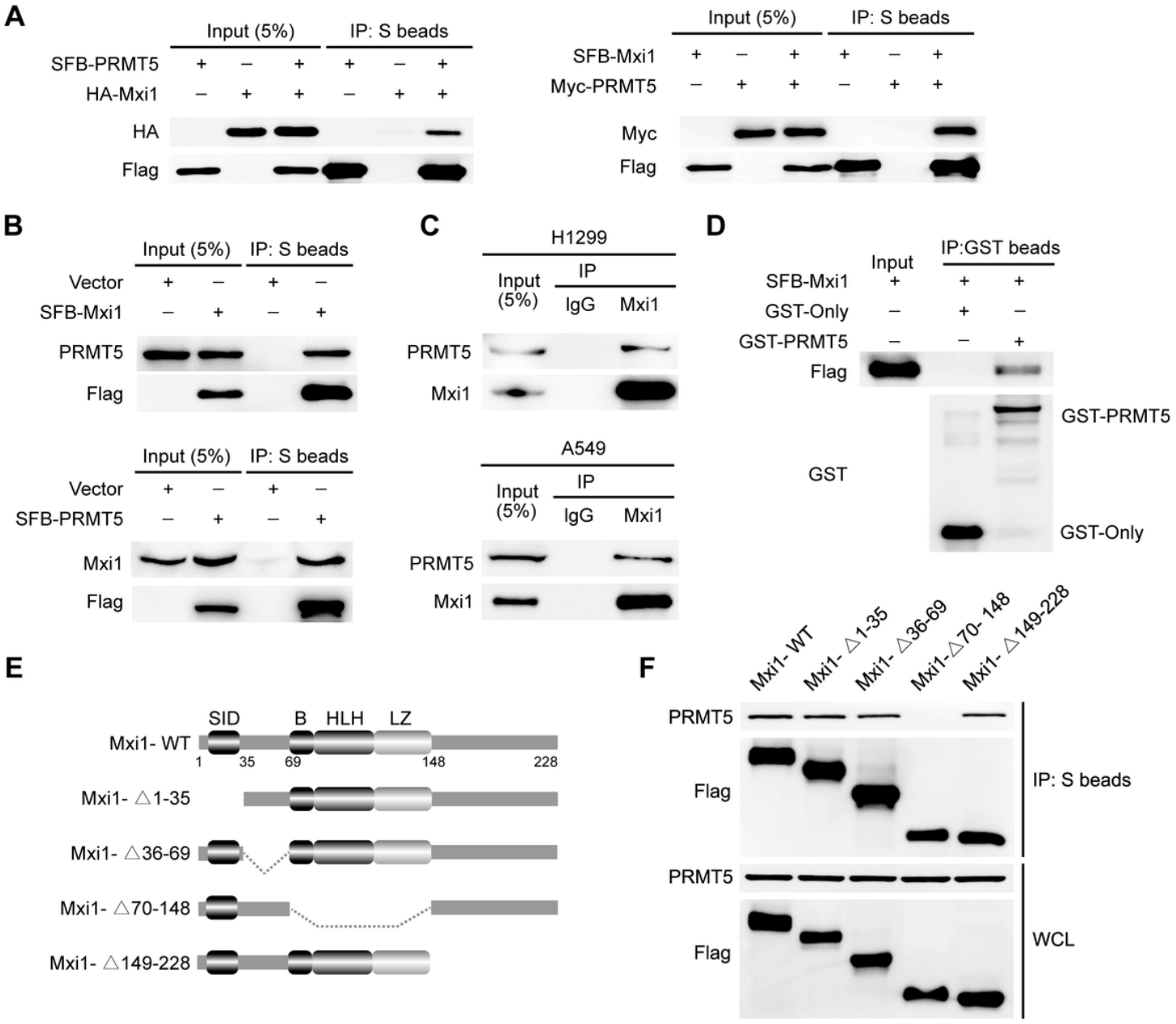

Figure 1

PRMT5 binds to Mxi1 in vitro and in vivo. A Co-immunoprecipitation of exogenously expressed Mxi1 and PRMT5 in HEK293T cells was presented (n = 3). B H1299 cells were transfected with the indicated constructs and treated with 10 mM MG132 for 4 h before harvesting (n = 3). C Endogenous Mxi1 interacted with PRMT5 in H1299 and A549 cells (n = 3). Rabbit IgG was used as the negative control. D Immunoblot analysis of GST pull-down precipitates from HEK293T cell lysates with ectopic expression of SFB-tagged Mxi1 incubated with bacterially purified recombinant GST or GST-PRMT5 protein (n = 3). E Schematic representation of various Mxi1 truncation mutants. F The B-HLH-LZ domain (70-148) of Mxi1 is required for its binding to PRMT5 (n = 3).

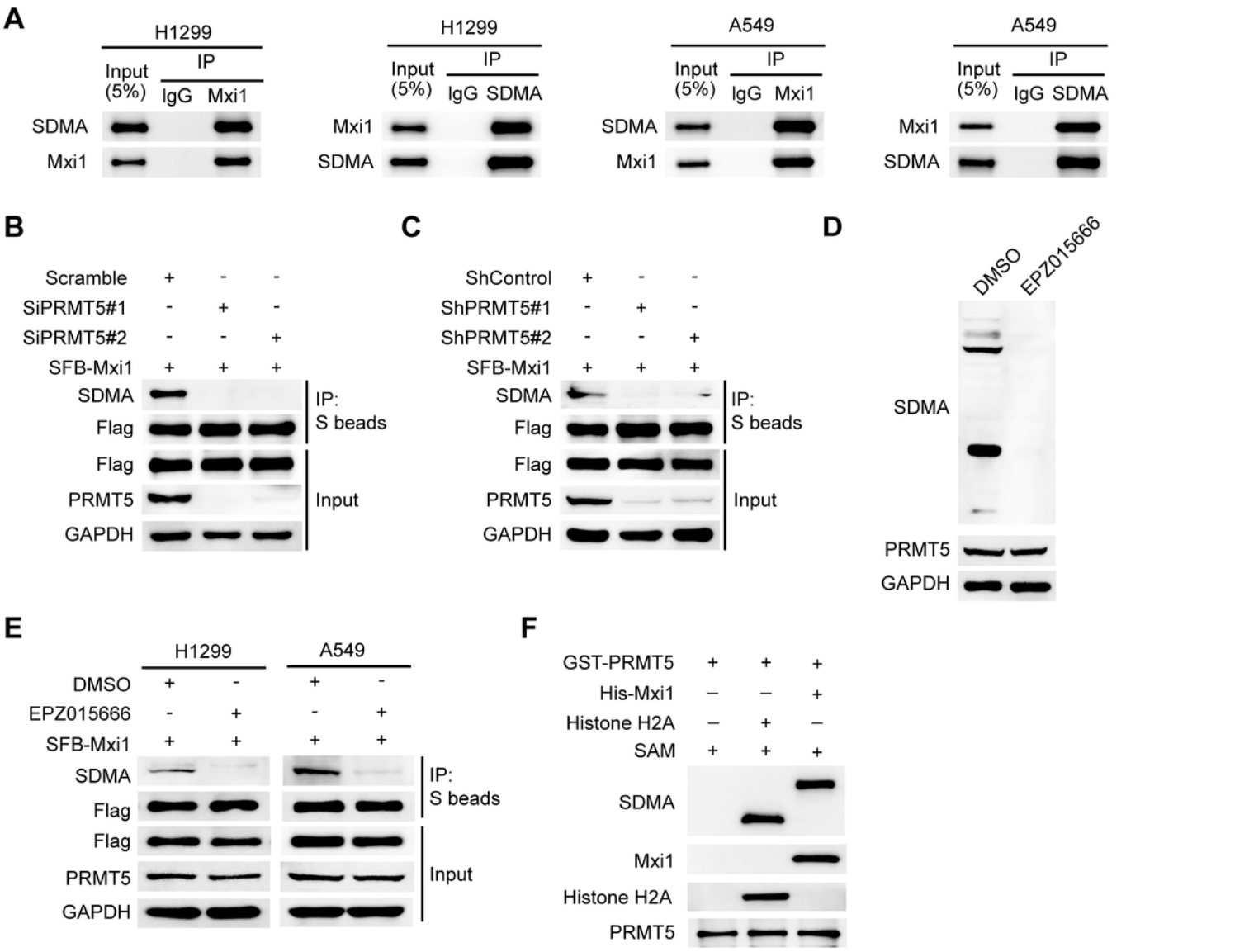

Figure 2

PRMT5 directly methylates Mxi1 in vitro and in vivo. A Co-immunoprecipitation of Mxi1 and symmetric dimethylarginine (SDMA) in H1299 and A549 cells revealed the symmetrical arginine dimethylation of Mxi1 (n = 3). B, C PRMT5 knockdown with specific siRNAs or shRNAs decreased Mxi1 symmetric arginine methylation. H1299 cells were transfected with the indicated siRNAs or shRNAs and plasmids, and then treated with 10 mM MG132 for 4 h before harvesting. co-IP experiments were performed with S beads and immunoblotting with an anti-SDMA antibody (n = 3). D Immunoblot analysis of total symmetrical arginine demethylation using an anti-SDMA antibody 48 h after H1299 cells were treated with 10 μM EPZ015666 (n = 3). E Immunoblot analysis of endogenous Mxi1 methylation in H1299 (10 μM for 48h) and A549 (25 μM for 72h) cells treated with EPZ015666 was shown (n = 3). F In vitro methylation assay with recombinant GST-PRMT5 and His-Mxi1 or histone H2A (positive control) proteins (n = 3).

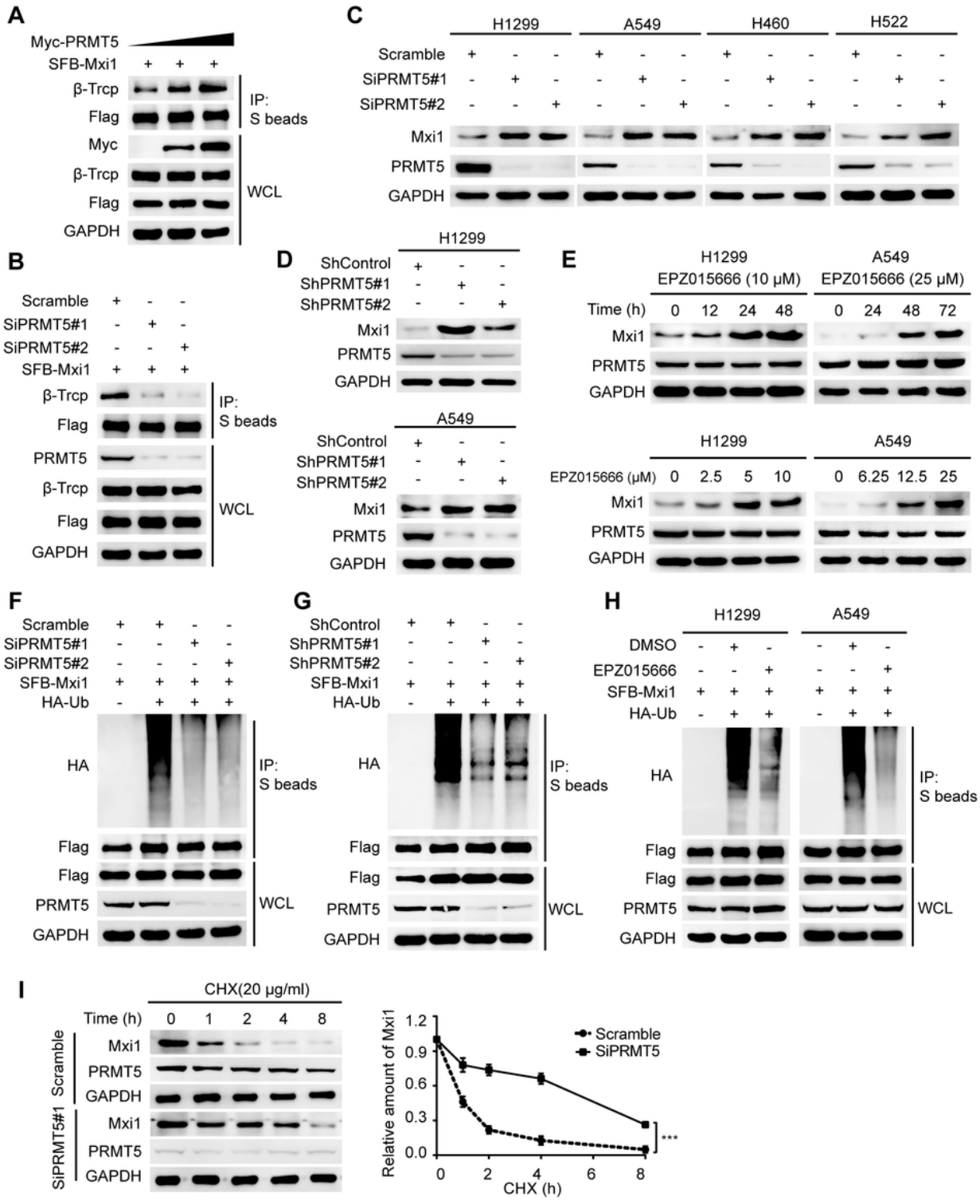

Figure 3

PRMT5 negatively controls Mxi1 protein stability by inducing Mxi1 polyubiquitination and degradation. A, B H1299 cells were transfected with the indicated constructs or siRNAs and treated with 10 mM MG132 for 4 h before harvesting. Co-immunoprecipitation experiments were conducted using S beads (n = 3). C Immunoblot analysis of endogenous PRMT5 and Mxi1 in H1299, A549, H460 and H522 cells transfected with the indicated siRNAs (n = 3). D Knockdown of PRMT5 using shRNAs led to increased Mxi1 protein

levels in H1299 and A549 cells (n = 3). E Immunoblot analysis of endogenous PRMT5 and Mxi1 in H1299 and A549 cells pretreated with EPZ015666 for the indicated times and concentrations (n = 3). F, G Depletion of endogenous PRMT5 decreased the polyubiquitination of Mxi1 in H1299 cells (f) and A549 cells (g) (n = 3). H Inhibition of PRMT5 with EPZ015666 (10 μM in H1299 cells for 48 h and 25 μM in A549 cells for 72 h) decreased Mxi1 polyubiquitination (n = 3). I Left panel: immunoblot analysis of the whole-cell lysates (WCL) derived from H1299 cells transfected with the indicated siRNAs. Forty-eight hours post transfection, cells were treated with cycloheximide (CHX, 20 μg/ml) for the indicated time. Right panel: Mxi1 protein levels were quantified (n = 3). ***P < 0.001.

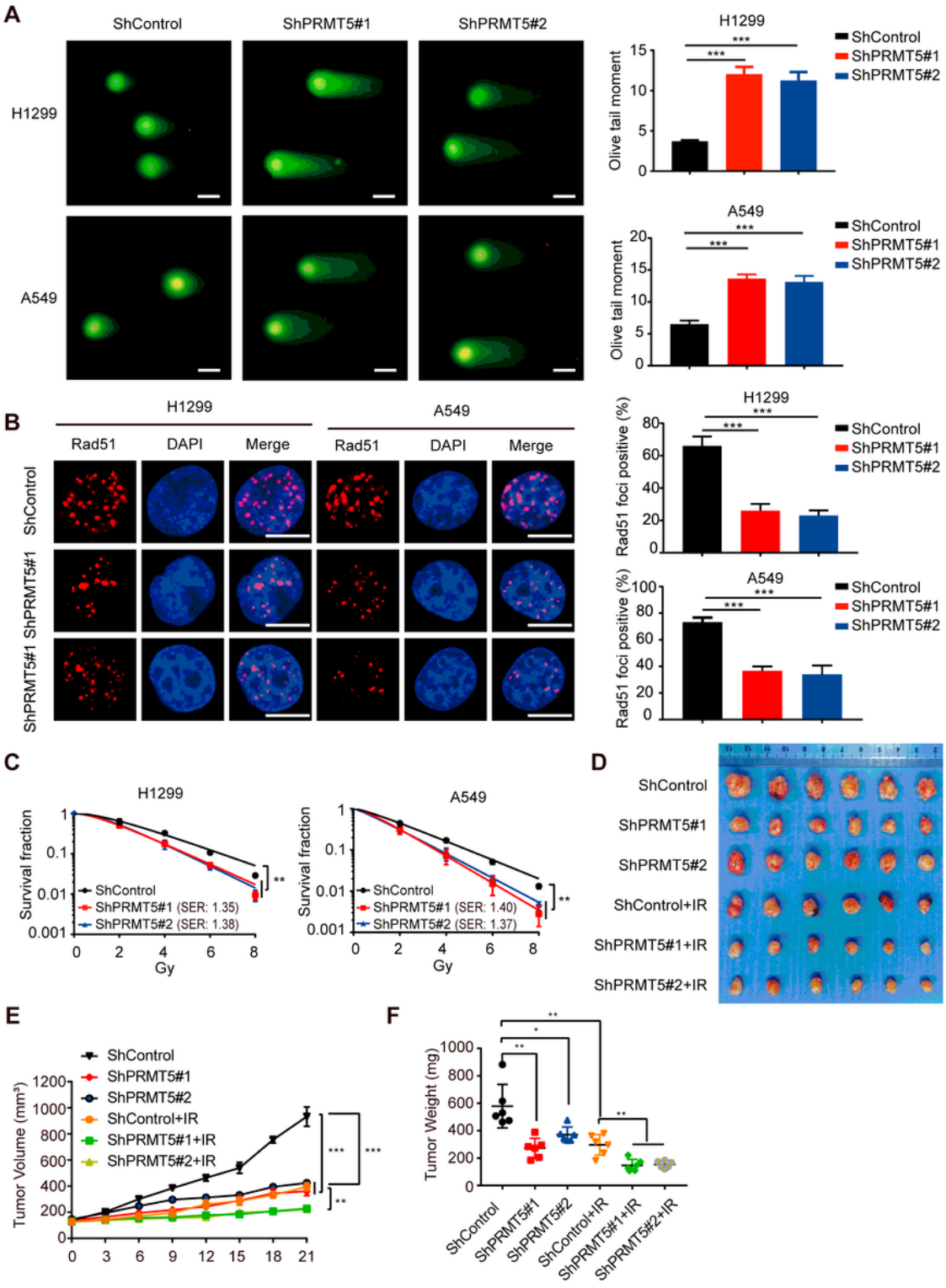

Figure 4

PRMT5 silencing enhances lung cancer radiosensitivity in vitro and in vivo. A Left panel: representative pictures of neutral comet assay of IR-induced DSBs. Scale bar, 10 μm. Right panel: quantification of comet tail moments.100 comet tails were assessed (the mean ± SEM; n = 3). ***P < 0.001. B Cells transfected with the indicated shRNAs were exposed to 6 Gy IR, and cells with >10 foci were quantified (n = 3). ***P < 0.001. C Loss of PRMT5 led to enhanced radiosensitivity (n = 3). SER: sensitization

enhancement ratio. **P < 0.01. D-F Effects of PRMT5 knockdown on tumor growth and weight in xenograft models (n = 6 mice/group). The growth curves (E) and weights (F) of the xenograft tumors in different groups are presented (the mean ± SEM). *P < 0.05, **P < 0.01, ***P < 0.001.

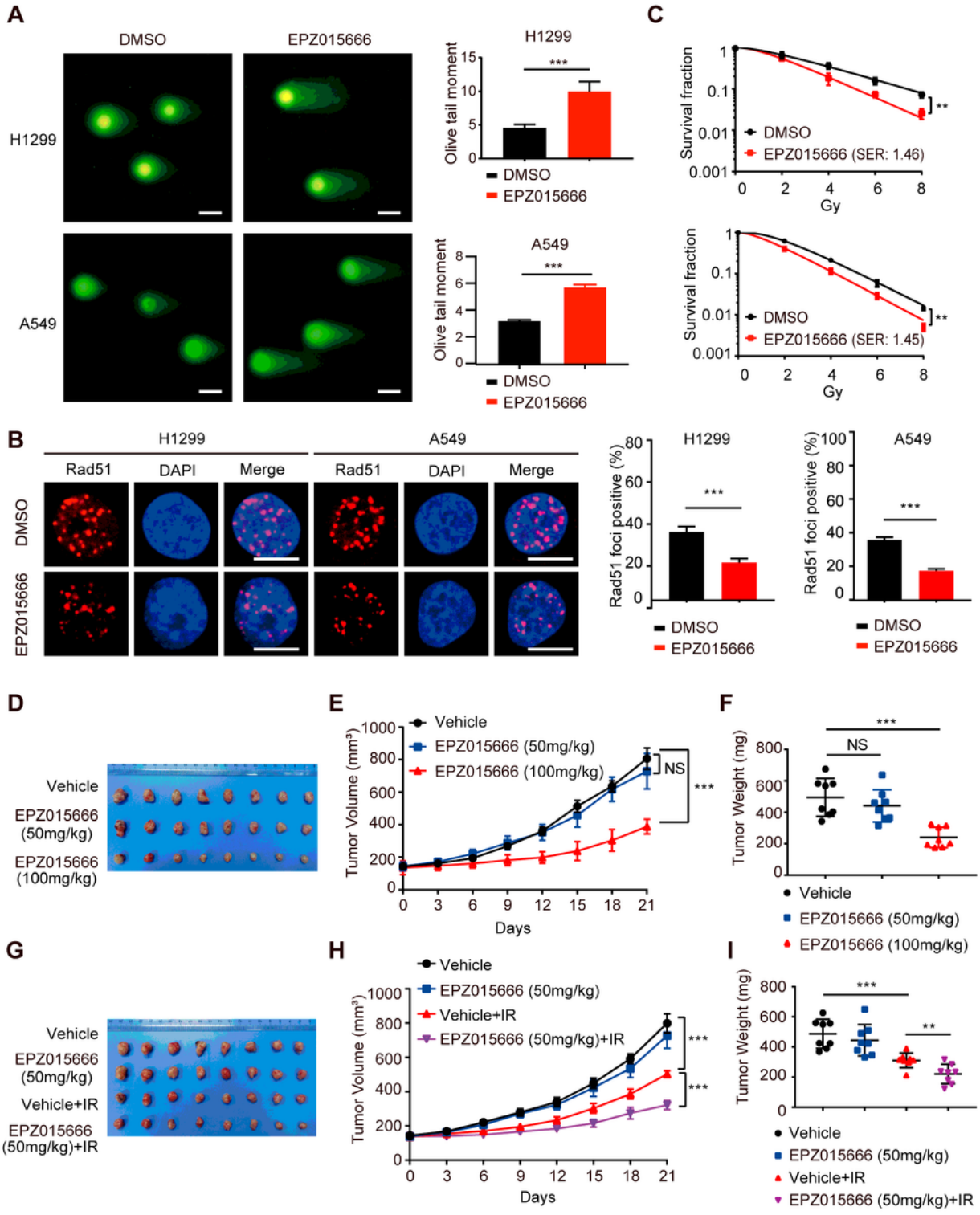

Figure 5

The PRMT5-specific inhibitor EPZ015666 is a potential radiosensitizer in lung cancer in vitro and in vivo. A EPZ015666 treatment (10 μM in H1299 cells for 48 h and 25 μM in A549 cells for 72 h) led to an

increased olive tail moment (n = 3). Scale bar, 10 μm. ***P < 0.001. B Cells pretreated with EPZ015666 were exposed to 6 Gy IR, and the cells with >10 foci were quantified (n = 3). ***P < 0.001. C Cells were treated with EPZ015666, and cell survival was determined by colony survival assay (n = 3). **P < 0.01. D-F Effects of EPZ015666 on tumor growth and weights in xenograft models. Nude mice were implanted with 5 × 106 A549 cells subcutaneously and then treated with 50 mg/kg or 100 mg/kg EPZ015666 by oral gavage every two days after xenograft volumes reached approximately 130 mm3 (n = 8 mice/group). Tumor growth was monitored for 21 days, and a growth curve was plotted (E). Xenografts were weighed and photographed on day 21. ***P < 0.001. G-I Tumor growth curves and weights of different groups were presented. Nude mice were injected with A549 cells and then treated only with IR, only with 50 mg/kg EPZ015666 or with 50 mg/kg EPZ015666 plus 10 Gy IR (n = 8 mice/group, the mean ± SEM). **P < 0.01, ***P < 0.001.

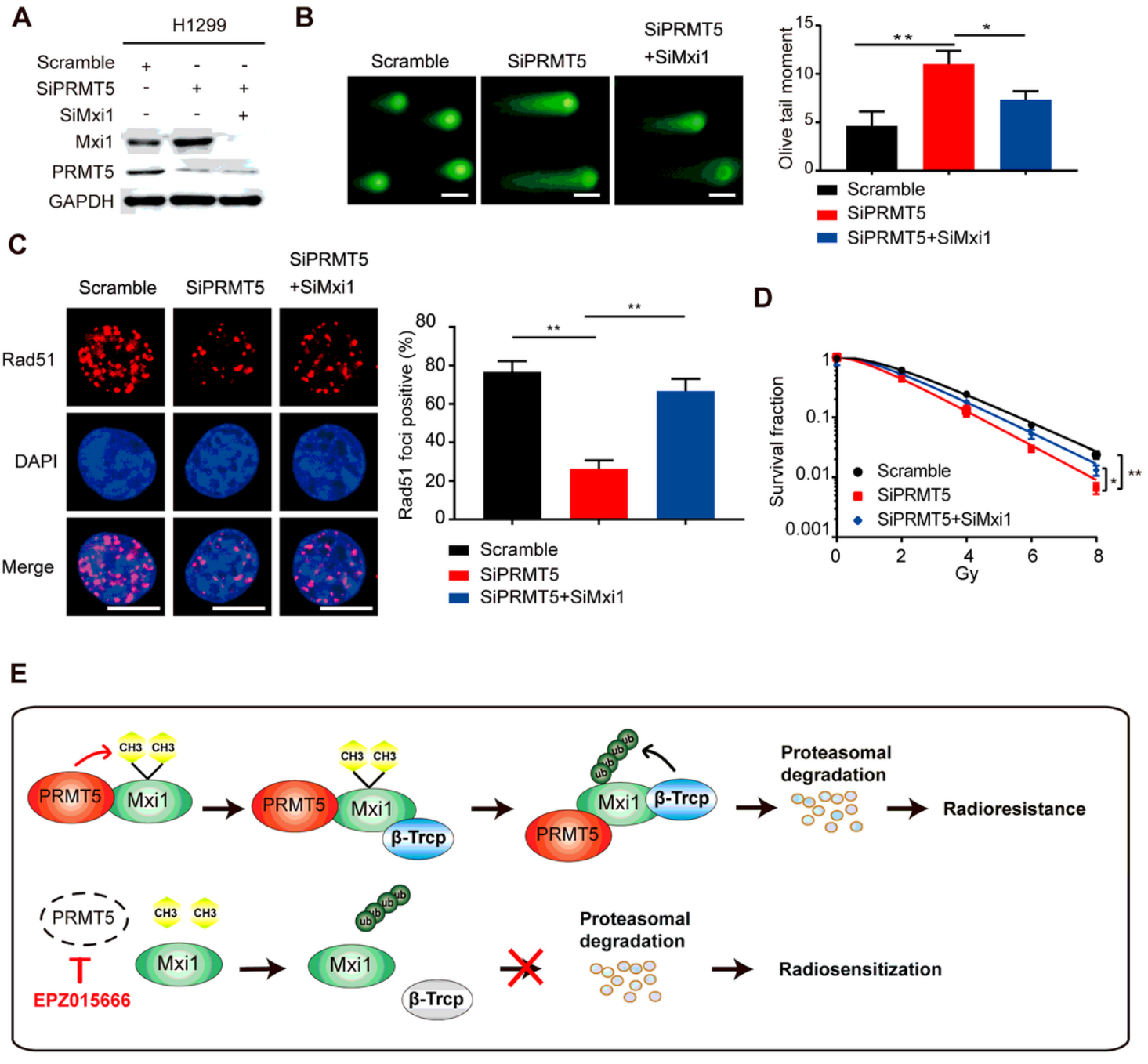

Figure 6

PRMT5 participates in lung cancer radioresistance in an Mxi1-dependent manner. A H1299 cells transfected with the indicated small interfering RNAs were harvested for analysis (n = 3). B Left panel: representative pictures showing the olive tail moment. Scale bar, 10 μm. Right panel: The olive tail moment was quantified (n = 3). *P < 0.05, **P < 0.01. C Left panel: representative pictures of Rad51 foci after exposure to 6 Gy irradiation (IR). Scale bar, 10 μm. Right panel: quantification of Rad51 foci in H1299 cells (n = 3). **P < 0.01. D H1299 cells were transfected with the indicated siRNAs, and cell survival was assessed by colony survival assay (n = 3). *P < 0.05, **P < 0.01. E Model showing the regulation of Mxi1 by PRMT5. PRMT5 binds to and symmetrically dimethylates Mxi1, which stimulates the interaction of Mxi1 and β-Trcp and the degradation of Mxi1, thus promoting radioresistance in lung cancer. Blockade of PRMT5 with EPZ015666 inhibits the methylation of Mxi1 and results in decreased binding of Mxi1 to β-Trcp, ultimately leading to the accumulation of Mxi1 and radiosensitization in lung cancer.